

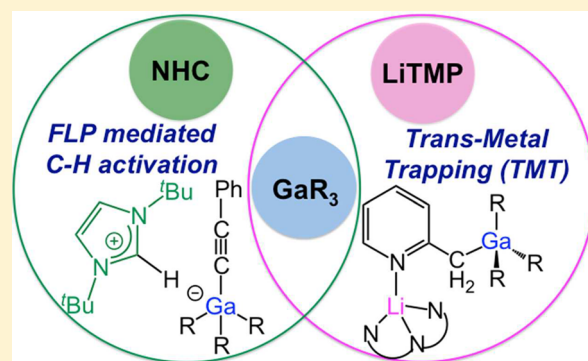
Trans-Metal-Trapping Meets Frustrated-Lewis-Pair Chemistry: Ga(CH₂SiMe₃)₃-Induced C–H Functionalizations

Marina Uzelac, Alan R. Kennedy,^{1b} and Eva Hevia*^{1b}

WestCHEM, Department of Pure and Applied Chemistry, University of Strathclyde, Glasgow G1 1XL, U.K.

S Supporting Information

ABSTRACT: Merging two topical themes in main-group chemistry, namely, cooperative bimetallics and frustrated-Lewis-pair (FLP) activity, this Forum Article focuses on the cooperativity-induced outcomes observed when the tris(alkyl)gallium compound GaR₃ (R = CH₂SiMe₃) is paired with the lithium amide LiTMP (TMP = 2,2,6,6-tetramethylpiperidide) or the sterically hindered N-heterocyclic carbene (NHC) 1,3-bis(*tert*-butyl)imidazol-2-ylidene (tBu). When some previously published work are drawn together with new results, unique tandem reactivities are presented that are driven by the steric mismatch between the individual reagents of these multicomponent reagents. Thus, the LiTMP/GaR₃ combination, which on its own fails to form a cocomplex, functions as a highly regioselective base (LiTMP)/trap (GaR₃) partnership for the metalation of N-heterocycles such as diazines, 1,3-benzoxazoles, and 2-picolines in a trans-metal-trapping (TMT) process that stabilizes the emerging sensitive carbanions. Taking advantage of related steric incompatibility, a novel monometallic FLP system pairing GaR₃ with tBu has been developed for the activation of carbonyl compounds (via C=O insertion) and other molecules with acidic hydrogen atoms such as phenol and phenylacetylene. Shedding new light on how these non-cocomplexing partnerships operate and showcasing the potential of gallium reagents to engage in metalation reactions or FLP activations, areas where the use of this group 13 metal is scant, this Forum Article aims to stimulate more interest and activity toward the advancement of organogallium chemistry.



INTRODUCTION

Deprotonative metalation is one of the most useful and widely used synthetic tools to functionalize organic molecules by transforming a relatively inert C–H bond into a more polar (and therefore reactive) metal–C bond.¹ Lithium alkyls, in the company of sterically demanding lithium amides (such as LiTMP, where TMP = 2,2,6,6-tetramethylpiperidide), commonly perform these reactions, although they can suffer from low functional-group tolerance and limited selectivity, imposing in many cases the use of extremely low temperatures to minimize possible side reactions or decomposition of the generated lithiated intermediates.² Overcoming some of these limitations, alternative multicomponent metalating reagents have been developed that in many cases pair metals of different polarities within the same molecule. Lochman–Schlosser superbases³ were the prototype of these bimetallic reagents, while Uchiyama's and Mongin's TMP/zincate complexes^{4,5} as well as LiCl-powered Knochel's turbo-Grignard reagents such as TMPMgCl·LiCl⁶ represent more recent examples.

Mulvey's structural and reactivity studies using amidoalkyl bimetallic combinations established the concept of alkali-metal-mediated metalation, where combining an alkali metal with a less electropositive metal such as magnesium, zinc, manganese(II), or iron(II) can promote unprecedented regioselective metalation, zincation, manganese, or ferration of aromatic

molecules usually inert toward single-metal magnesium,⁷ zinc,⁸ manganese(II),⁹ or iron(II)¹⁰ reagents. This usually occurs by the formation of “ate” complexes, resulting from cocomplexation of two distinct organometallic compounds, e.g., alkali metal and a second less electropositive metallic center (such as zinc or magnesium) with a variety of anionic ligands (e.g., alkyl, amido, or alkoxy groups) to give a single bimetallic entity (Figure 1a), where the metal with stronger Lewis acidity can accept more (Lewis) basic ligands. Such mixing of the metals and ligands, where the anionic charge is localized on the part of the molecule containing the more electronegative metal, can have cooperative consequences, in transferring the high reactivity of the alkali-metal component to the less polar metal while retaining its greater selectivity and functional group compatibility, enabling direct metal–H exchange at room temperature (contrasting with the low-temperature protocols required with RLi reagents).

Furthermore, in some cases, unique synergic regioselectivities are achievable, promoting the polymetalation of substrates at remote positions, again attributed to the synchronized cooperation of metals within the bimetallic reagent. Recent

Special Issue: Advances in Main-Group Inorganic Chemistry

Received: March 3, 2017

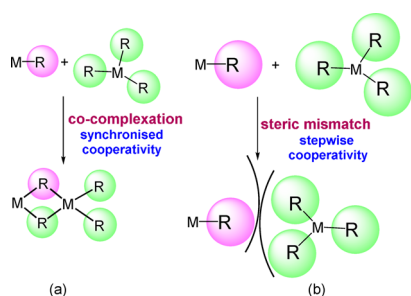
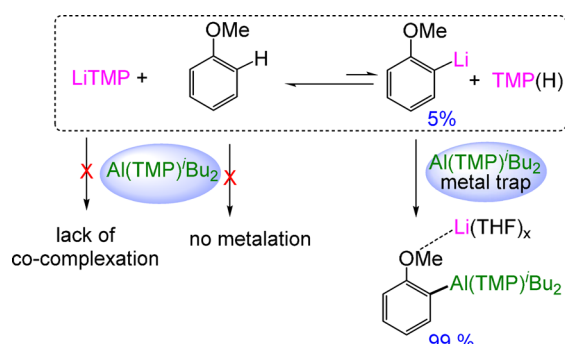


Figure 1. Contrast between synchronized (a) and stepwise (b) cooperativity.

examples include regioselective dimagnesiumation of *N,N*-dimethylaniline¹¹ and the *N*-heterocyclic carbene (NHC) 1,3-bis(2,6-diisopropylphenyl)imidazol-2-ylidene (IPr),¹² where the supramolecular structure of the mixed sodium/magnesium base templates the regioselectivity of the deprotonation reaction.¹³

While most of such studies have focused on divalent metals, work on trivalent group 13 metals aluminum and gallium has evidenced that cooperative effects can also result from multicomponent solutions containing two separate metal species, which fail to form an ate (co)complex (Figure 1b). In these cases, a bimetallic cooperativity operates in tandem, with one metal (e.g., lithium, the base) performing metalation while another (e.g., aluminum, the trap) drives the equilibrium toward the target product, transforming low-yielding lithiations into quantitative reactions. For example, collaborating with Mulvey, we recently showed that the LiTMP-induced ortho metalation of anisole can be dramatically increased from 5% of lithiated anisole to 99% of aluminated product by adding Al(TMP)^tBu₂ as a metal trap, in a process driven by the strong carbophilicity and bulk of the aluminum reagent via a trans-metal-trapping (TMT) procedure (Scheme 1).¹⁴

Scheme 1. TMT Procedure for Ortho Metalation of the Benchmark Substrate Anisole¹⁴

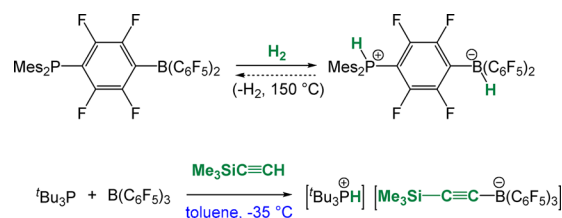


This stepwise cooperativity of the LiTMP/Al(TMP)^tBu₂ partnership relies primarily on the lack of cocomplexation between the two homometallic reagents as a result of their steric incompatibility. This bimetallic system has been successfully employed to execute metalations under mild conditions of a variety of molecules including 1,3-dimethoxybenzene,¹⁵ *N,N*-diisopropylbenzamide,¹⁵ ferrocene,¹⁶ or tetrahydrofuran (THF).¹⁷

This TMT concept of steric mismatch between the single components of a mixed-metal system, which leads to a remarkable amplified metalation of a substrate, bears a

similarity with frustrated-Lewis-pair (FLP) chemistry. Being a powerful methodology for small-molecule activation that has already found numerous applications in catalysis, FLP chemistry is based on the steric incompatibility of a Lewis acid (LA) and a Lewis base (LB) to form a stable donor/acceptor complex, enabling cooperative behaviors with added substrates through unique reaction pathways.¹⁸ Some key landmarks in this young but rapidly evolving field include dihydrogen activation¹⁹ and hydrogenation catalysis,²⁰ as well as CO/CO₂ reductions,²¹ the capture of greenhouse gases,²² and C–H activation processes (Scheme 2).²³ Although the

Scheme 2. Selected Examples of FLPs Employed for Heterolytic Cleavage of Hydrogen^{19a} and C–H Bond Activation



most powerful FLPs to date rely on the use of sterically hindered, electron-rich organophosphines as the LB component,^{18,19a,20,24} NHCs, which have a myriad of applications in their own right,²⁵ are increasingly attracting attention in this field. While sharing many coordination features with phosphines, NHCs offer greater potential for subtle variations of their steric/electronic properties.^{18d,25,26} In addition to their tuneability, the *N*-substituents are responsible for inducing “steric pressure” toward the LA component by being directed toward the carbene lone pair.^{18d} Although most systems use a boron complex as the LA component,¹⁸ the use of other group 13 elements, in particular aluminum,²⁷ is steadily growing in popularity with some other recent examples reported using gallium²⁸ and indium.^{28e} Interestingly, although NHCs cannot activate hydrogen on their own, cyclic and acyclic (alkyl)-(amino)carbenes can operate as single-site molecules for the activation of hydrogen under mild conditions.²⁹ Similarly, many of the heavier main-group multiple-bonded and open-shell species can be described as unimolecular FLPs (although typically not referred as such) because they contain donor and acceptor sites capable of activating small molecules.³⁰

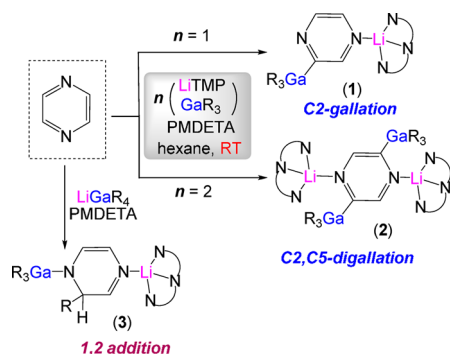
Building on recent advances from our group, this Forum Article brings together for the first time cooperative bimetallics and FLP chemistry, reporting on noncomplexing metal compound/metal compound and metal compound/ligand partnerships. Using the tris(alkyl)gallium GaR₃ (R = CH₂SiMe₃) as a connecting thread between these two fundamentally important areas, herein we compare their applications for the functionalization of several organic substrates. By pairing GaR₃ with the sterically demanding lithium amide LiTMP or the NHC 1,3-bis(*tert*-butyl)imidazol-2-ylidene (I^tBu), we utilize steric mismatches to promote unique tandem reactivities, which to date are unprecedented in organogallium chemistry.

TMT and Sequential Metalation. Building on our previous LiTMP/Al(TMP)^tBu₂ work,^{14–17} we extended TMT approaches to the heavier group 13 metal, gallium. Possessing a higher electronegativity than aluminum, with the ability of forming even less polarized metal–C bonds, this system has the

potential to sedate and stabilize unstable incipient carbanions arising from the deprotonation of N-heterocyclic molecules. NMR studies assessing cocomplexation between LiTMP, with the tris(alkyl)gallium complex GaR_3 ($\text{R} = \text{CH}_2\text{SiMe}_3$) containing bulky and thermally stable monosilyl groups, revealed that they fail to form a bimetallic complex. TMT was then successfully used for regioselective metalation of challenging sensitive, unactivated diazines in hydrocarbon solutions as well as the N–S heterocycle benzothiazole.³¹ Metalated intermediates of all of these reactions were isolated and structurally defined, showing remarkable stability. Remarkably, we can carry out these reactions under mild reaction conditions, using stoichiometric amounts of metalating reagents, and at room temperature, contrasting with previous reports that require large excesses of LiTMP (up to 4 equiv) as well as strict temperature control (-78°C) to avoid decomposition of the lithio intermediates, and even under these restrictive conditions, yields tend to be moderate.³²

Scheme 3 summarizes some of our investigations of the

Scheme 3. Contrasting Approaches in the Synthesis of Mono- and Digallated Pyrazine and Addition Product³¹



metalation of pyrazine.³¹ Reacting 1 equiv of a $\text{GaR}_3/\text{LiTMP}$ mixture using hexane as the solvent and the tridentate donor PMDETA (as a crystallization aid) afforded the 2-monogallated complex [1-(PMDETA)Li-3-(GaR_3) $\text{C}_4\text{H}_3\text{N}_2$] (1; Scheme 3). Furthermore, to show stoichiometric control, two hydrogen atoms can be removed from the 2 and 5 positions of pyrazine when the base/trap/substrate ratio was doubled to 2:2:1 (2 in Scheme 3). Contrastingly, when pyrazine was tackled by the related homoalkyllithium gallate [LiGaR_4], metalation was inhibited, promoting instead the regioselective addition of an alkyl group to one α -carbon of the heterocycle (3 in Scheme 3).

When the inherent instability of α -metalated pyrazines is pondered, the isolation of compounds 1 and 2 as stable crystalline solids at room temperature may seem surprising; however, their molecular structures provide important clues that help us to understand their stability. Figure 2 shows that two well-defined bonding modes are established for each metal, minimizing repulsions between the electron clouds of the nitrogen lone pair (tied up in forming dative bonds with lithium) and the negative charge of the carbanion, which is further stabilized by forming a more covalent and less polarized Ga–C bond, being also protected by the steric shelter of the bulky monosilyl groups.

Extension of the TMT approach to pyridazine, pyrimidine, and benzothiazole led to the isolation of complexes 4–6, respectively (Figure 3).³¹

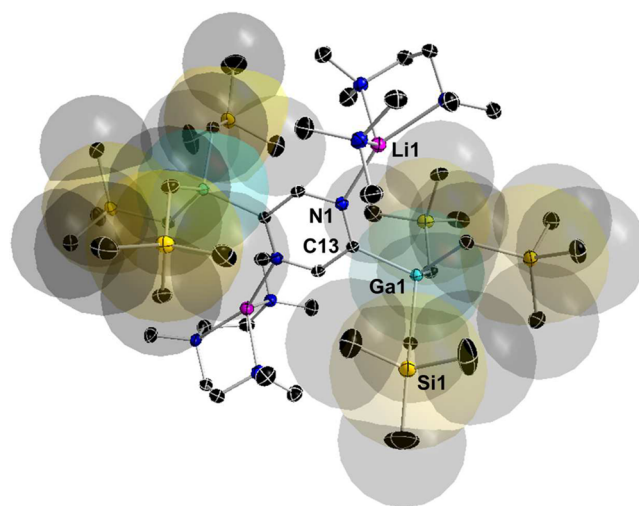


Figure 2. Molecular structure of 2 with 50% probability displacement ellipsoids and with superimposed translucent space-filling van der Waals surfaces for a probe of 1 Å radius for GaR_3 fragment. All hydrogen atoms have been omitted for clarity.

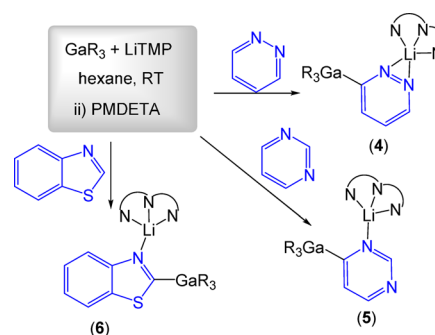


Figure 3. Products of TMT-executed metalations of pyridazine, pyrimidine, and benzothiazole.³¹

Interestingly, for pyridazine, it was found that introducing the gallium trap to the heterocycle prior to the addition of LiTMP led to noticeably better regioselective control, driving the reaction toward the formation of C3-metalated product 4. In addition, while ring-closed 2-lithiated benzothiazole derivatives coexist in solution at room temperature with ring-opened forms,³³ 6 is stable in solution and no equilibration with its metallo(2-isocyano)thiophenolate isomer could be detected.

Extending the scope of TMT to other N-heterocyclic molecules containing less acidic protons, here we report our findings on the exploration of deprotonation of N-methylbenzimidazole (BIm) and 2-picoline. When the same conditions as those for the metalation of diazines were applied, LiTMP and GaR_3 were added to a solution of the relevant substrate in hexane at room temperature. The addition of PMDETA produced [2-(GaR_3)-3-{Li(PMDETA)}- $\text{C}_6\text{H}_4\text{N}_2\text{CNCMe}$] (7) and [(PMDETA)Li(2- CH_2 -pyridine)- GaR_3] (8) as colorless crystals in high (isolated) yields of 81% and 79%, respectively (Scheme 4).

X-ray crystallography confirmed gallation of these heterocyclic substrates, with BIm metalated at its C2 position (Figure 4), whereas 2-picoline undergoes lateral deprotonation (Figure 5). Within contact-ion-pair structures, both lithium and gallium centers in 7 and 8 display tetrahedral geometries, with lithium attached to four nitrogen atoms (three from PMDETA and one

Scheme 4. Products of Lithium–Gallium TMT of BIm and 2-Picoline

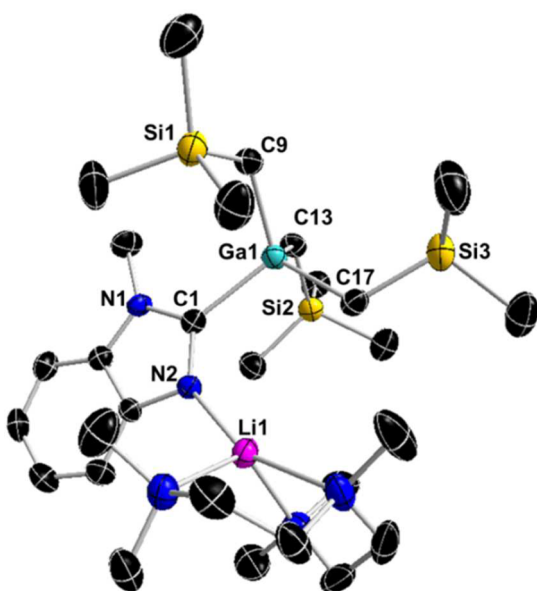
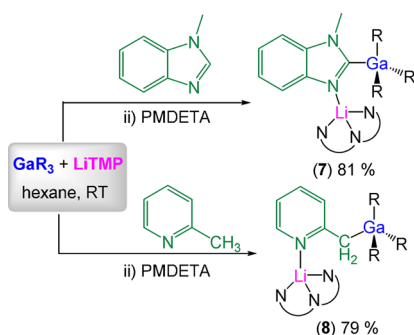


Figure 4. Molecular structure of 7 with 50% probability displacement ellipsoids. All hydrogen atoms have been omitted for clarity. Selected bond distances (Å) and angles (deg): Ga1–C1 2.054(3), Ga1–C9 2.030(3), Ga1–C13 2.032(3), Ga1–C17 2.001(3), Li1–N2 2.063(6), Li1–N3 2.191(6), Li1–N4 2.302(6), Li1–N5 2.119(7); C1–Ga1–C13 104.24(13), C1–Ga1–C9 110.60(13), C1–Ga1–C17 108.78(12), C9–Ga1–C13 110.15(13), C17–Ga1–C13 112.64(14), C17–Ga1–C9 110.29(13), N2–Li1–N5 109.2(3), N2–Li1–N3 105.4(3), N5–Li1–N3 121.3(3), N2–Li1–N4 157.7(3), N5–Li1–N4 82.6(2), N3–Li1–N4 82.7(2).

from the metalated heterocycle), whereas the GaR_3 fragment coordinates to the carbon atom that has experienced deprotonation, showing the same distinct Li–N/Ga–C bonding preferences previously discussed for 2. The Ga– sp^2 C(BIm) bond distance of 2.054(3) Å is in excellent agreement with the similar Ga– sp^2 C(btz) bond of 2.062(3) Å previously found in 6.³¹ While 2-picolyl anions can exhibit different coordination modes to metals depending on the degree of delocalization of the negative charge into the ring,³⁴ the geometrical parameters of 8 suggest that this fragment is best described as a carbanionic ligand, forming a Ga– CH_2 bond [Ga–C13 2.099(4) Å in Figure 5] that is comparable to the remaining Ga– C_{alkyl} bonds in 8 (mean 2.027 Å). This particular bonding mode is further supported by the Li–N bond distance [Li1–N1 2.055(8) Å in Figure 5], which is noticeably longer than the corresponding bond found in the enamido complex

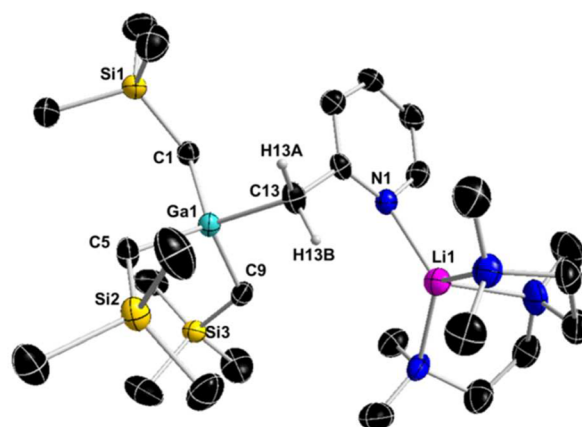


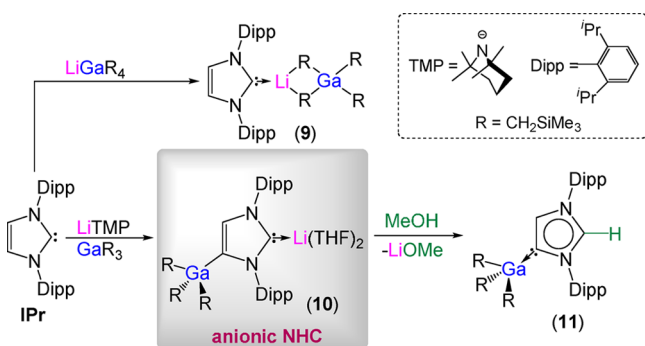
Figure 5. Molecular structure of 8 with 50% probability displacement ellipsoids. All hydrogen atoms and the minor disorder of the PMDETA ligand have been omitted for clarity. Selected bond distances (Å) and angles (deg): Ga1–C1 2.025(4), Ga1–C5 2.030(4), Ga1–C9 2.025(4), Ga1–C13 2.099(4), Li1–N1 2.055(8), Li1–N2 2.178(8), Li1–N3 2.145(8), Li1–N4 2.11(2); C1–Ga1–C13 108.29(18), C1–Ga1–C9 111.06(18), C1–Ga1–C5 112.49(18), C9–Ga1–C13 102.59(19), C5–Ga1–C13 108.95(18), C5–Ga1–C9 112.88(19), N1–Li1–N4 108.6(5), N1–Li1–N3 121.8(4), N4–Li1–N3 125.5(5), N1–Li1–N2 123.4(4), N4–Li1–N2 84.6(4), N3–Li1–N2 84.4(3).

[(2- CH_2 -pyridine)Li(PMDETA)] [Li–N 2.002(4) Å]^{34e} and is similar to that found in 7 [Li1–N2 2.063(6) Å].³⁵

Solubility in deuterated THF enabled 7 and 8 to be characterized using ^1H and ^{13}C NMR spectroscopy (see the Experimental Section and Supporting Information). For 7, the most diagnostic resonance in the ^{13}C NMR spectrum appears at 188.8 ppm for the benzimidazole C2 ring carbon that was metalated and is now attached to gallium, which is significantly downfield compared to the C2 resonance observed in free BIm (142.7 ppm).³⁶ Contrasting with Boche's previous NMR studies,³³ which revealed that at room temperature 2-lithio-*N*-methylbenzimidazole undergoes partial ring opening in deuterated THF, the ^1H and ^{13}C NMR spectra of 7 displayed well-resolved signals with no detectable resonances that could be assigned to a ring-opened α -isocyanomethylamide species. Lateral metalation of 2-picoline in 8 was confirmed by the presence of four multiplets in the aromatic region of the ^1H NMR spectrum (from 6.5 to 8.1 ppm) along with a singlet at 1.79 ppm for the CH_2 -Ga moiety, whereas the ^{13}C NMR spectrum displayed an informative signal at 30.8 ppm attributed to the CH_2 -Ga fragment.

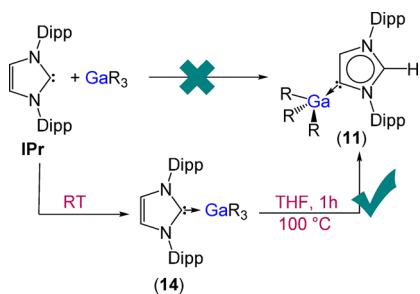
Multicomponent bimetallic reagents have also shown great promise in deprotonating NHCs. Some of our recent work has shown that sodium magnesiate¹² and zincates³⁷ can promote direct mangesiation (or zincation) at the imidazole backbone of unsaturated carbenes such as IPr. In contrast, LiGaR_4 does not promote metalation of this carbene, but the coordination adduct [IPr–LiGaR₄] (9; Scheme 5).³⁸ However, the TMT approach led to the isolation of heteroleptic lithium gallate (THF)₂Li[·C{[N(2,6-*i*Pr₂C₆H₃)₂CHCGaR₃}] (10), where the metals connect via an anionic NHC that coordinates via its normal C2 position to lithium and its abnormal C4 position to gallium.³⁹ Electrophilic interception studies of 10 using methanol,³⁸ methyl triflate,³⁸ or Me_3SiCl ⁴⁰ afforded $\alpha\text{IPr-GaR}_3$ (11), $[\text{CH}_3\text{C}\{[\text{N}(2,6-*i*\text{Pr}_2\text{C}_6\text{H}_3)_2\text{CHCGa}(\text{CH}_2\text{SiMe}_3)_3\}]$ (12), and $[\text{Me}_3\text{SiC}\{[\text{N}$

Scheme 5. Synthesis of Homoleptic Tetraalkyl Gallate 9, Heteroleptic Gallate 10, and Abnormal Adduct 11



($2,6\text{-}i\text{Pr}_2\text{C}_6\text{H}_3$) $_2\text{CHCGa}(\text{CH}_2\text{SiMe}_3)_3$] (**13**), respectively. Their structures were elucidated by X-ray crystallography, revealing the preference of the anionic NHC ligand present in **10** to react with electrophiles at its C2 position, leaving its C4 position intact; thus, all of these reactions introduce a new method to access abnormal NHC/Ga complexes.

While using this bimetallic metalation/electrophilic quenching approach allowed isolation of **11**, treating IPr with GaR₃ in hexane at room temperature furnished the normal isomer IPr-GaR₃ (**14**; Scheme 6).³⁸ It is rare to find examples where both

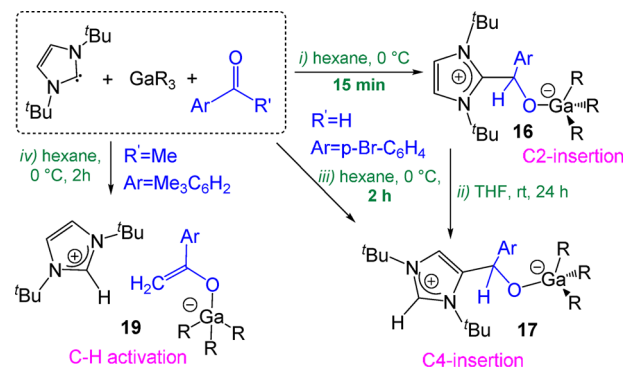
Scheme 6. Synthesis of Normal Adduct 14 and Its Thermal Isomerization into the Abnormal Isomer 11³⁸

normal and abnormal metal NHC complexes have been isolated or structurally characterized.^{38,41,42} Within iron chemistry, Layfield has elegantly demonstrated thermal isomerization of IPr-Fe(HMDS)₂ to *a*IPrFe(HMDS)₂ (3 h, 110 °C, toluene), suggesting that formation of the abnormal NHC complex is thermodynamically driven by the relief of steric hindrance around the metal center.⁴² Motivated by this work, we assessed the thermal stability of **14** towards isomerization. These studies revealed that the abnormal isomer **11** can be obtained in 77% yield by heating a THF solution of **14** at 100 °C for 1 h.³⁸

Combining NMR spectroscopic and kinetic studies with DFT calculations intimated that the isomerization occurred via a dissociative mechanism, akin to mechanisms proposed in NHC/borane FLP systems,^{19a,43} evidencing the importance of the substituent steric bulk on the nitrogen atoms of the NHC ligand. Thus, whereas both **11** and **14** are stable and easily accessible, steric incompatibility prevents GaR₃ and I^tBu from forming a stable normal adduct, rendering instead *a*I^tBu-GaR₃ (**15**) at room temperature.³⁸ Encouraged by these initial findings hinting at the potential FLP reactivity that this NHC/Ga system may exhibit, we have probed the reactivity of some

single-metal non-cocomplexing partnerships to promote C–H and C=O bond activation of a range of organic molecules.^{28d}

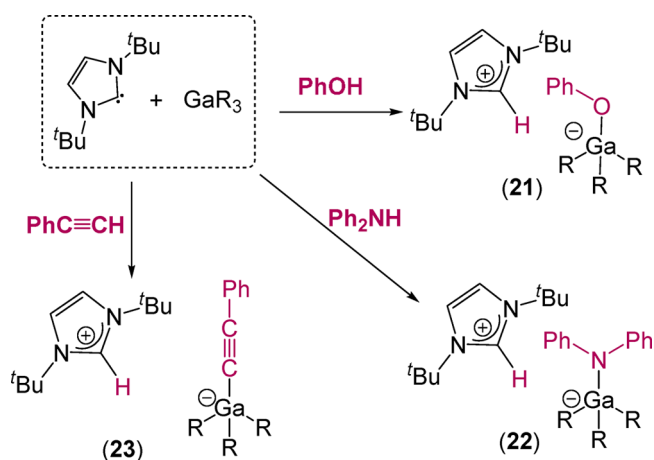
FLP Activation of Organic Molecules by NHC/GaR₃ Pairings. Demonstrating that GaR₃ is a viable effective LA for promoting small-molecule-activation processes when paired with sterically demanding I^tBu, we have recently reported the reduction of aldehydes, by insertion into the C=O functionality at the C2 carbene position, affording zwitterionic compounds such as I^tBuCH(*p*-Br-C₆H₄)OGaR₃ (**16**; Scheme 7i).^{28d} Reflecting the cooperativity of the I^tBu/GaR₃ pair,

Scheme 7. Contrasting Reactivities of I^tBu/GaR₃ Mixtures with Various Carbonyl Compounds^{28d}

neither component is able to activate aldehydes on their own. Interestingly, solution studies, supported by theoretical calculations, reveal that **16** is the kinetic product of the addition across the C=O functionality and over time (24 h, room temperature) evolves into its thermodynamic product **17** (Scheme 7ii), resulting from formal insertion into the C=O group at the C4 carbene position (Scheme 7iii).^{28d} These findings showed that I^tBu can effectively act as a LB via both its normal (C2) and its abnormal (C4) positions. The reactivity of the NHC/Ga pair was further tested against ketones, and it was found that reduction of the carbonyl moiety takes place only in the case of electrophilic α,α -trifluoroacetophenone furnishing *a*I^tBuC(Ph)(CF₃)OGaR₃ (**18**), while less electrophilic benzophenone remains intact and the deactivation complex *a*I^tBu-GaR₃ (**15**) is detected instead.^{28d} Interestingly, with enolizable ketones such as 2,4,6-trimethylacetophenone, a different FLP reactivity pattern was revealed, affording mixed imidazolium gallate salts [$\{\text{I}^t\text{BuH}\}^+\{(\text{Ar})\text{C}(\text{=CH}_2)\text{OGaR}_3\}^-$] (**19**; Ar = Me₃C₆H₂) as a result of a C–H activation process (Scheme 7iv). This reactivity was also seen for other unsaturated organic substrates bearing α -acidic hydrogen atoms such as diphenylacetone nitrile affording [$\{\text{I}^t\text{BuH}\}^+\{\text{Ph}_2\text{C}=\text{C}=\text{NGaR}_3\}^-$] (**20**).^{28d}

Here we extend the reactivity of this NHC/Ga FLP to other molecules containing protic hydrogen atoms, susceptible to undergoing C–H and X–H (X = O, N) activation. We start with phenol whose deprotonation can be achieved by either of the two components on their own (i.e., I^tBu or GaR₃), as evidenced by the mixture of products obtained upon the addition of phenol to a hexane suspension of the I^tBu/GaR₃ pair. However, if phenol was added to the hexane suspension of I^tBu, followed by the addition of GaR₃, a more controlled O–H bond cleavage occurred, affording [$\{\text{I}^t\text{BuH}\}^+\{\text{GaR}_3\text{OPh}\}^-$] (**21**) in a 76% yield (Scheme 8). Selective formation of **21** was evident from its ¹H NMR spectrum in THF-*d*₈, which unambiguously revealed a 1:3 ratio of phenoxy (6.16, 6.52, and

Scheme 8. FLP Activation of Phenol, Diphenylamine, and Phenylacetylene



6.79 ppm) to monosilyl (-0.78 and -0.07 ppm) anions, as well as three characteristic singlets for the imidazolium cation at 8.82, 7.75, and 1.3 ppm for the N_2CH , NCH and ${}^t\text{Bu}$ groups, respectively.

Encouraged by these results, we next took on more challenging substrates, probing the reactivity of the ${}^t\text{Bu}/\text{GaR}_3$ pair toward diphenylamine (Ph_2NH) and phenylacetylene ($\text{PhC}\equiv\text{CH}$). Following the same order of addition as that for **21**, $\text{N}-\text{H}$ and $\text{C}-\text{H}$ activations of diphenylamine and phenylacetylene were accomplished, affording $[\{\text{I}^t\text{BuH}\}^+\{\text{GaR}_3\text{NPh}_2\}^-]$ (**22**) and $[\{\text{I}^t\text{BuH}\}^+\{\text{GaR}_3\text{CCPh}\}^-]$ (**23**) in 38% and 78% yields, respectively (Scheme 8). The modest isolated yield of **22** prompted us to inspect the filtrate more closely; thus, ${}^1\text{H}$ NMR spectra revealed unreacted diphenylamine and the formation of **15**. This finding suggests that, even at 0°C , the competing NHC rearrangement process that deactivates the NHC/Ga pair can still take place. It should also be noted that secondary amines have previously been successfully employed as LBs in FLPs for hydrogen activation.⁴⁴ Thus, Rieger and co-workers paired $\text{B}(\text{C}_6\text{F}_5)_3$ with TMPH (TMPH = 2,2,6,6-tetramethylpiperidine) or ${}^i\text{Pr}_2\text{NH}$,^{44a} whereas Pápai and co-workers showed that, in certain cases (depending on the steric hindrance), a borane/imine combination after cleaving hydrogen and affording borane/amine adduct can react further with more hydrogen to afford ammonium hydroborate salt.^{44b}

Compounds **21–23** could all be isolated as crystals and their structures elucidated by X-ray crystallography (Figures 6 and 7). These displayed similar general structural features of a salt-like ion-pair structure comprising a protonated imidazolium cation charge-balanced by a heteroleptic gallate anion. The gallate anion contains three monosilyl groups and the relevant anionic fragment stemming from $\text{X}-\text{H}$ activation ($\text{X} = \text{O}, \text{N}, \text{C}$) of the substrate, that is, aryloxo PhO^- (**21**), amido Ph_2N^- (**22**), or alkynyl $\text{PhC}\equiv\text{C}^-$ (**23**) ligands.

All three structures show a distorted tetrahedral gallium geometry, as evidenced by $\text{C}-\text{Ga}-\text{X}$ bond angles ($\text{X} = \text{C}, \text{O}, \text{N}$) ranging from $95.4(2)^\circ$ to $115.6(2)^\circ$ [mean angle 108.87° in **21**, 109.33° in **22**, and 109.36° in **23**]. The $\text{Ga}-\text{C}_{\text{alkyl}}$ distances (Table S3) show little variation [mean 2.016 \AA in **21**, 2.023 \AA in **22**, and 2.022 \AA in **23**] and agree well with the values of other tetracoordinated gallium species.^{38,45} The $\text{Ga}-\text{O}$ bond distance in **21** [$1.981(4)\text{ \AA}$] shows good agreement with literature values for gallium complexes containing terminal

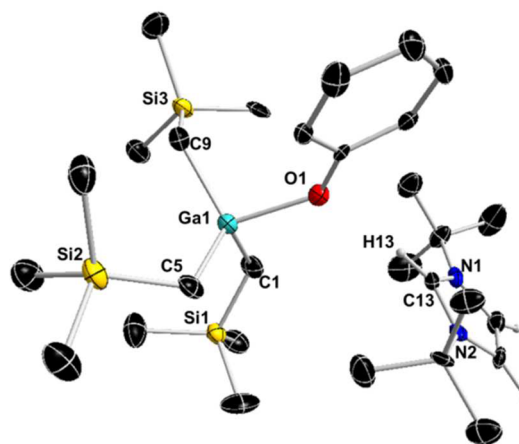


Figure 6. Molecular structure of **21** with 50% probability displacement ellipsoids. All hydrogen atoms except those on the imidazole ring have been omitted for clarity. Selected bond distances (\AA) and angles (deg): $\text{Ga1}-\text{O1}$ $1.981(4)$, $\text{Ga1}-\text{C1}$ $2.000(6)$, $\text{Ga1}-\text{C5}$ $2.029(6)$, $\text{Ga1}-\text{C9}$ $2.020(5)$; $\text{C1}-\text{Ga1}-\text{O1}$ $95.4(2)$, $\text{O1}-\text{Ga1}-\text{C9}$ $102.7(2)$, $\text{C1}-\text{Ga1}-\text{C9}$ $117.8(3)$, $\text{C5}-\text{Ga1}-\text{O1}$ $107.3(2)$, $\text{C5}-\text{Ga1}-\text{C1}$ $115.6(2)$, $\text{C5}-\text{Ga1}-\text{C9}$ $114.4(2)$, $\text{N1}-\text{C13}-\text{N2}$ $109.2(5)$.

alkoxy ligands.^{45b} The $\text{Ga}-\text{N}$ bond length of $2.0150(17)\text{ \AA}$ in **22** is only slightly shorter than the $\text{Ga}-\text{N}$ distance reported for the lithium gallate incorporating the $[\{\text{Ph}_3\text{Ga}(\mu\text{-NMe}_2)\text{-GaPh}_3\}^-]$ anion [$\text{Ga}-\text{N}$ $2.051(1)\text{ \AA}$],⁴⁶ consistent with the terminal versus bridging mode of the amido ligand. The $\text{Ga}-\text{C1}$ bond in **23** of $2.031(3)\text{ \AA}$ is only slightly elongated in comparison with the $\text{Ga}-\text{C}$ bond distance in anionic $[\{\text{Ga}(\text{CCSiMe}_3)_3(2,6\text{-}^i\text{Pr}_2\text{C}_6\text{H}_3\text{N}(\text{SiMe}_3))\}^-]$ (average $\text{Ga}-\text{C} = 1.969\text{ \AA}$).^{47a}

Multinuclear NMR analysis confirmed that the solid structures exhibited by **21–23** are preserved in $\text{THF}-d_8$ solutions (see the Experimental Section and Supporting Information). Two informative singlets in a 2:1 ratio at 7.86 and 8.80 ppm for the CHN and NCHN protons, respectively, evidenced the presence of the imidazolium cation. The ${}^{13}\text{C}$ NMR spectrum of **23** displayed two resonances at 104.7 and 105.4 ppm, which can be assigned to the α and β positions, respectively, of the alkynyl fragment.⁴⁷

The formation of **23**, where the LB ${}^t\text{Bu}$ deprotonates phenylacetylene while the three monosilyl groups attached to gallium remain intact, contrasts with the results observed when $\text{IPr}-\text{GaR}_3$ (**14**), containing a less sterically demanding NHC, is reacted with phenylacetylene. Here one R group on gallium acts as a base, to give $\text{IPr}-\text{GaR}_2(\text{C}\equiv\text{CPh})$ (**24**), with IPr behaving as an ancillary ligand. This reactivity is similar to that described previously by Mitzel and co-workers for the reaction of GaMe_3 and 4-ethynyl-2,6-lutidine, where the metalation of terminal alkyne by GaMe_3 occurs with concomitant release of methane.⁴⁸ Very recently, Uhl and co-workers demonstrated that gallium hydrazides can act as active Lewis pairs for the cooperative $\text{C}-\text{H}$ bond activation of phenylacetylene⁴⁹ where the steric bulk of the tris(alkyl)gallium reagent dictates the extent of metalation.⁵⁰ Complexes **23** and **24** illustrate how the reactivity of these new NHC/Ga FLP systems can be finely tuned by small modifications on the steric bulk of the components, in this case the LB (Scheme 9).

Isolated in a 55% yield, the NHC complex was crystallographically characterized. The molecular structure of **24** is comparable to that of **14**, where a Lewis adduct is formed by

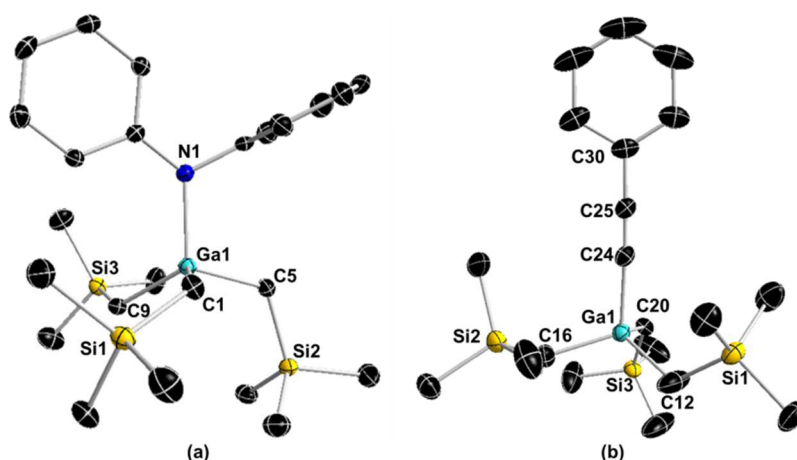
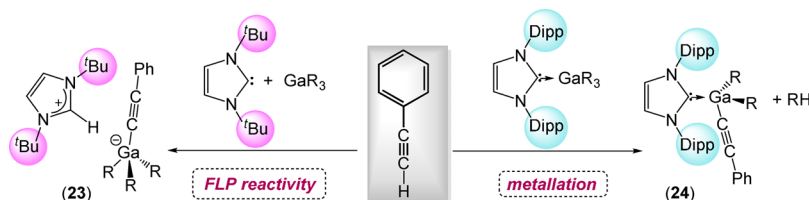


Figure 7. (a) Anionic moiety of the molecular structure of **22** with 50% probability displacement ellipsoids. All hydrogen atoms have been omitted for clarity. Selected bond distances (Å) and angles (deg): Ga1–N1 2.0150(17), Ga1–C1 2.031(2), Ga1–C5 2.022(2), Ga1–C9 2.015(2); C1–Ga1–N1 103.88(8), N1–Ga1–C9 113.35(8), C1–Ga1–C9 113.31(9), C5–Ga1–N1 103.26(8), C5–Ga1–C1 109.25(9), C5–Ga1–C9 112.95(9). (b) Anionic moiety of molecular structure of **23** with 50% probability displacement ellipsoids. All hydrogen atoms and disorder components in two CH_2SiMe_3 groups have been omitted for clarity. Selected bond distances (Å) and angles (deg): Ga1–C12 2.011(3), Ga1–C16 2.038(4), Ga1–C20 2.018(4), Ga1–C24 2.031(3), C24–C25 1.205(4); C12–Ga1–C20 107.74(18), C12–Ga1–C24 110.84(13), C20–Ga1–C24 103.46(13), C12–Ga1–C16 115.44(18), C20–Ga1–C16 110.07(16), C24–Ga1–C16 108.62(14).

Scheme 9. Contrasting Reactivities of Different NHC/ GaR_3 Mixtures with Phenylacetylene: FLP-Induced Deprotonation versus Direct Gallation



the coordination of a neutral gallium fragment to the normal (C2) position of a neutral IPr carbene. As previously seen in **14**, the gallium center adopts a distorted tetrahedral geometry; however, the distortion is less pronounced, as evidenced by the C–Ga–C bond angles ranging from 100.09(14) to 116.63(14)°. This is most probably due to the relief of steric crowding by the replacement of one CH_2SiMe_3 group with the $\text{C}\equiv\text{CPh}$ group, causing a shortening of the Ga–C_{NHC} bond [Ga–C9 2.104(4) Å in Figure 8 vs 2.1960(16) Å in **14**]. The Ga–C_{alkynyl} (Ga–C1 in Figure 8) distance of 1.954(4) Å is slightly more contracted than that observed in **23** [2.031(3) Å], consistent with the neutral constitution of the former versus the gallate of the latter. Regarding its NMR characterization, while **23** is very insoluble in C_6D_6 , **24** displayed an excellent solubility in this low-coordinating solvent. The most informative resonances in the ^{13}C NMR spectrum are C_{NHC}–Ga at 179.4 ppm, which is upfield-shifted compared to the free carbene, and the two alkynyl resonances at 106.9 ppm (Ga–C \equiv CPh) and 112.5 ppm (GaC \equiv CPh) (see the Experimental section and Supporting Information for details).

CONCLUSION AND OUTLOOK

Advancing the applications of organogallium complexes for the functionalization of organic substrates, this Forum Article discusses cooperative behaviors observed when pairing tris-(alkyl) gallium GaR_3 (R = CH_2SiMe_3) with the utility lithium amide LiTMP or the sterically hindered NHC tBu. When two topical areas of main-group chemistry, namely, cooperative

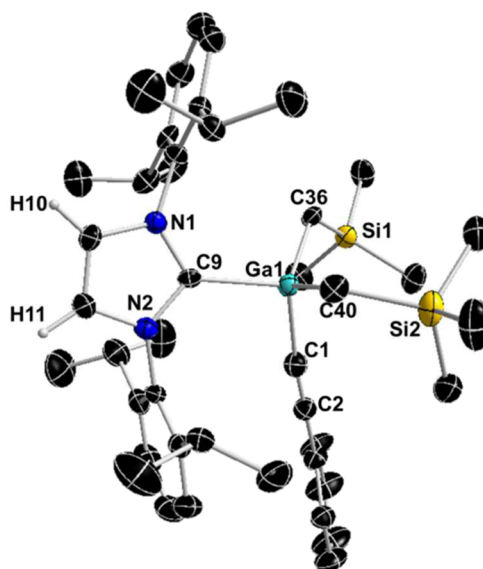


Figure 8. Molecular structure of **24** with 50% probability displacement ellipsoids. All hydrogen atoms except those on the imidazole ring and the minor disorder in the alkyne ligand have been omitted for clarity. Selected bond distances (Å) and angles (deg): Ga1–C1 1.954(4), Ga1–C9 2.104(4), Ga1–C36 1.997(3), Ga1–C40 1.997(3), C1–C2 1.203(5); C1–Ga1–C40 110.43(15), C1–Ga1–C36 111.94(15), C40–Ga1–C36 116.63(14), C1–Ga1–C9 105.44(14), C40–Ga1–C9 100.09(14), C36–Ga1–C9 111.16(13), N1–C9–N2 103.7(3), Ga1–C1–C2 174.6(4).

bimetallics and FLP activity, are merged, the reactivity of these systems is controlled by the steric mismatches between their individual components.

Thus, when stepwise metal compound/metal compound cooperativity was exploited, sterically hindered LiTMP and GaR₃ were found not to undergo cocomplexation to form a weakly basic, coordinatively saturated gallate. Instead, operating in a tandem manner, this bimetallic mixture can be used to effect room temperature deprotonation of sensitive heterocycles, revealing new regioselectivities and reactivity patterns that cannot be accomplished by the monometallic reagents alone. We describe this stepwise cooperativity as TMT approaches, which exploit both the strong basicity of LiTMP (which carries out deprotonation of the substrate) and the pronounced carbophilicity of GaR₃ (which traps and stabilizes the incipient anion generated via metalation), facilitating challenging functionalizations to be accomplished with high selectivity under mild conditions at room temperature in a hydrocarbon solvent. We have also introduced two new examples of gallium TMT chemistry by structurally defining compounds **7** and **8** resulting from the regioselective deprotonation of Blm and 2-picoline, respectively.

When such steric incompatibility is exported in the domain of monometallic chemistry, a novel FLP system pairing the same organogallium reagent with the bulky NHC has been developed for small-molecule activation. When GaR₃ as a LA was effectively combined with the LB I^tBu, X–H (X = O, N, C) activation of molecules bearing acidic hydrogen atoms such as phenol or phenylacetylene was achieved, in a controlled manner and under mild reaction conditions to yield novel mixed-imidazolium gallate complexes **21** and **23**, respectively. The subtle steric effects operating in these processes have been demonstrated by switching from I^tBu to the related NHC IPr, which suppresses the FLP reactivity in contact with phenylacetylene, demoting the NHC from acting as a base to becoming a spectator ligand, affording NHC complex **24**, where phenylacetylene has been metalated by one R group on gallium.

The chemistry developed for the organogallium reagent, presented in this paper, highlights stepwise cooperative processes based either on two metal reagents or on a single-metal reagent combined with a special ligand. By shedding new light on how these noncocomplexing partnerships operate and showcasing the potential of gallium reagents to engage in metalation reactions or FLP activations, areas where the use of this metal is scant, this Forum Article aims to stimulate more interest and activity toward the advancement in organogallium chemistry, bridging the gap in practical utility and knowledge between gallium and its neighbors aluminum and boron.

EXPERIMENTAL SECTION

All reactions were carried out using standard Schlenk and glovebox techniques under an inert atmosphere of argon. Solvents (THF, hexane, benzene, and toluene) were dried by heating to reflux over sodium benzophenone ketyl and distilled under nitrogen prior to use. NMR spectra were recorded on a Bruker DPX 400 MHz spectrometer, operating at 400.13 MHz for ¹H and 100.62 MHz for ¹³C{¹H}. 1-Methylbenzimidazole, phenylacetylene, phenol, and diphenylamine were purchased from Sigma-Aldrich Chemicals or Alfa Aesar and used as received. 2-Picoline was dried by heating to reflux over calcium hydride, distilled under nitrogen, and stored over activated 4 Å molecular sieves prior to use. [Ga(CH₂SiMe₃)₃],⁵¹ I^tBu,⁵² and LiTMP⁵³ were prepared according to literature methods and stored

and handled under an inert atmosphere because of their air sensitivity (I^tBu) and pyrophoricity (Ga(CH₂SiMe₃)₃ and LiTMP).

Synthesis of [3-(PMDETA)Li-2-(GaR₃)C₈H₇N₂] (7). To a suspension of LiTMP (0.074 g, 0.5 mmol) and Ga(CH₂SiMe₃)₃ (0.165 g, 0.5 mmol) in hexane (10 mL) was added via solid addition tube at room temperature 1 equiv of 1-methylbenzimidazole (66 mg, 0.5 mmol). A very fine white suspension was obtained and stirred for 2 h at room temperature, after which PMDETA was added (0.11 mL, 0.5 mmol), inducing a stronger precipitation. Gentle heating afforded a solution that, upon slow cooling, deposited X-ray suitable crystals (0.26 g, 81%). Anal. Calcd for C₂₉H₆₃GaLiN₅Si₃: C, 54.19; H, 9.88; N, 10.90. Found: C, 54.32; H, 10.06; N, 11.09. ¹H NMR (298 K, THF-*d*₈) δ –0.77 (6H, s, CH₂SiMe₃), –0.15 (27H, s, Si(CH₃)₃), 2.15 (12H, s, N(CH₃)₂), 2.21 (3H, s, NCH₃), 2.32 (4H, mult, NCH₂CH₂N), 2.43 (4H, mult, NCH₂CH₂N), 3.84 (3H, s, ArNCH₃), 7.03 (2H, mult, ArCH), 7.31 (1H, mult, ArCH), 7.37 (1H, mult, ArCH). ¹³C{¹H} NMR (298 K, THF-*d*₈): δ –0.5 (CH₂SiMe₃), 3.1 (Si(CH₃)₃), 33.0 (NCH₃), 43.4, 46.2, 57.3, 58.8 (PMDETA), 109.5 (CHAr), 116.3 (CHAr), 120.9 (CHAr), 137.6 (CAr), 145.4 (CAr), 188.8 (CGa). ⁷Li NMR (298 K, THF-*d*₈, reference LiCl in D₂O at 0.00 ppm): δ 3.24.

Synthesis of [1-(PMDETA)Li-2-CH₂(GaR₃)C₅H₄N] (8). To a suspension of LiTMP (0.074 g, 0.5 mmol) and Ga(CH₂SiMe₃)₃ (0.165 g, 0.5 mmol) in hexane (10 mL) was added via syringe at room temperature 1 equiv of 2-picoline (46 mg, 49 μL, 0.5 mmol). A very fine orange suspension was obtained and stirred for 1 h at room temperature, after which PMDETA was added (0.11 mL, 0.5 mmol), inducing the formation of red oil separating from a yellow solution. The mixture was placed at –20 °C, affording X-ray suitable crystals (0.24 g, 79.5%). Anal. Calcd for C₂₇H₆₂GaLiN₄Si₃: C, 53.71; H, 10.35; N, 9.28. Found: C, 52.60; H, 9.81; N, 9.78. ¹H NMR (298 K, C₆D₆): δ –0.44 (6H, s, CH₂SiMe₃), 0.45 (27H, s, Si(CH₃)₃), 1.54–1.66 (8H, br mult, NCH₂CH₂N), 1.77 (12H, s, NCH₃), 2.07 (3H, s, NCH₃), 2.12 (2H, s, ArCH₂), 6.35 (1H, t, ArCH), 7.09 (1H, t, ArCH), 7.23 (1H, d, ArCH), 7.35 (1H, d, ArCH). ¹³C{¹H} NMR (298 K, C₆D₆): δ 0.7 (CH₂SiMe₃), 3.9 (Si(CH₃)₃), 38.9 (ArCH₂Ga), 45.2, 45.5, 53.1, 56.7 (PMDETA), 113.9 (CHAr), 122.7 (CHAr), 135.4 (CHAr), 145.1 (CHAr), 174.1 (CAr). ⁷Li NMR (298 K, C₆D₆, reference LiCl in D₂O at 0.00 ppm): δ 0.75. ¹H NMR (298 K, THF-*d*₈): δ –1.14 (2H, s, CH₂SiMe₃), –1.02 (4H, s, CH₂SiMe₃), –0.19 (9H, s, Si(CH₃)₃), –0.10 (18H, s, Si(CH₃)₃), 1.79 (2H, s, ArCH₂), 2.18 (12H, s, NCH₃), 2.24 (3H, s, NCH₃), 2.35 (4H, mult, NCH₂CH₂N), 2.45 (4H, mult, NCH₂CH₂N), 6.59 (1H, t, ArCH), 6.77 (1H, d, ArCH), 7.30 (1H, t, ArCH), 8.03 (1H, d, ArCH). ¹³C{¹H} NMR (298 K, THF-*d*₈): δ 0.4 (CH₂SiMe₃), 3.1 (Si(CH₃)₃), 3.7 (CH₂SiMe₃), 4.1 (Si(CH₃)₃), 30.9 (ArCH₂Ga), 43.6, 46.1, 56.7, 56.8 (PMDETA), 114.8 (CHAr), 122.7 (CHAr), 135.9 (CHAr), 147.0 (CHAr), 173.8 (CAr). ⁷Li NMR (298 K, THF-*d*₈, reference LiCl in D₂O at 0.00 ppm): δ 0.14–1.15 (br).

Synthesis of [(I^tBuH)]⁺{(PhOGaR₃)[–]} (21). To a cooled solution of Ga(CH₂SiMe₃)₃ (0.165 g, 0.5 mmol) in 10 mL of hexane) was added phenol (47 mg, 0.5 mmol), followed by I^tBu (0.09 g, 0.5 mmol), and the obtained white suspension was stirred for 2 h at 0 °C. The suspension was concentrated to approximately 5 mL in volume, and 2 mL of toluene was added. Gentle heating afforded a solution that, upon cooling, deposited colorless X-ray-quality crystals (230 mg, 76%), which were isolated by filtration. Anal. Calcd for C₂₉H₅₉N₂O₃Si₃Ga: C, 57.50; H, 9.82; N, 4.62. Found: C, 57.85; H, 9.46; N, 5.33. ¹H NMR (298 K, THF-*d*₈): δ –0.78 (6H, s, CH₂SiMe₃), –0.07 (27H, s, Si(CH₃)₃), 1.63 (18H, s, C(CH₃)₃), 6.16 (1H, t, *p*-ArCH), 6.52 (2H, d, *o*-ArCH), 6.79 (2H, t, *m*-ArCH), 7.75 (2H, s, imidazole backbone CH), 8.82 (1H, s, C₂H). ¹³C{¹H} NMR (298 K, THF-*d*₈): δ 2.7 (CH₂SiMe₃), 3.5 (Si(CH₃)₃), 29.8 (C(CH₃)₃), 61.2 (C(CH₃)₃), 112.4 (*p*-ArCH), 121.0 (*o*-ArCH), 121.7 (imidazole backbone CH), 132.2 (NCHN), 128.6 (*m*-ArCH), 168.7 (ArC_{ipso}).

Synthesis of [(I^tBuH)]⁺{(Ph₂NGaR₃)[–]} (22). To a cooled solution of Ga(CH₂SiMe₃)₃ (0.165 g, 0.5 mmol) in 10 mL of hexane) was added diphenylamine (85 mg, 0.5 mmol), followed by I^tBu (0.09 g, 0.5 mmol), and the obtained white suspension was stirred for 2 h at 0 °C. The suspension was concentrated to approximately 5 mL in volume, and 2 mL of toluene was added. Gentle heating afforded a solution that, upon cooling, deposited colorless X-ray-quality crystals (130 mg,

38%). Anal. Calcd for $C_{35}H_{64}N_3Si_3Ga$: C, 61.74; H, 9.47; N, 6.17. Found: C, 58.18; H, 9.58; N, 5.22. Elemental and NMR spectroscopic analyses are consistent with the sample containing impurities such as unreacted diphenylamine. While 1H monitoring of this reaction in THF- d_8 showed the formation of **22** as a pure compound (72% conversion; see Figures S13 and S14 in the Supporting Information), NMR analyses of crystalline samples consistently showed the presence of variable amounts of NHPH₂ and another unknown gallium species containing R groups.

1H NMR (298 K, THF- d_8): δ -0.80 (6H, s, CH_2SiMe_3), -0.09 (27H, s, $Si(CH_3)_3$), 1.57 (18H, s, $C(CH_3)_3$), 6.39 (t, 2H, *p*-ArCH), 6.75 (d, 4H, *o*-ArCH), 6.89 (t, 4H, *m*-ArCH), 7.55 (2H, s, imidazole backbone), 8.32 (1H, s, C2H). $^{13}C\{^1H\}$ NMR (298 K, THF- d_8): δ 2.8 (CH_2SiMe_3), 3.8 ($Si(CH_3)_3$), 29.9 ($C(CH_3)_3$), 60.9 ($C(CH_3)_3$), 115.6 (*p*-ArCH), 123.9 (*o*-ArCH), 121.1 (imidazole backbone CH), 128.3 (*m*-ArCH), 136.1 (NCHN), 157.2 (ArC_{ipso}).

Synthesis of $[[t^iBuH]^+PhCGaR_3]^-$ (23**).** To a cooled solution of $Ga(CH_2SiMe_3)_3$ (0.165 g, 0.5 mmol) in 10 mL of hexane was added phenylacetylene (51 mg, 55 μ L, 0.5 mmol), followed by t^iBu (0.09 g, 0.5 mmol). The obtained white, thick suspension was stirred for 2 h at 0 °C, after which the solvent was exchanged in vacuo for benzene (5 mL). Gentle heating afforded a solution that, upon cooling, afforded X-ray-quality crystals (240 mg, 78%). Anal. Calcd for $C_{31}H_{60}GaN_2Si_3$: C, 60.66; H, 9.69; N, 4.56. Found: C, 60.43; H, 9.73; N, 4.84. 1H NMR (298 K, THF- d_8): δ -1.01 (6H, s, CH_2SiMe_3), -0.02 (27H, s, $Si(CH_3)_3$), 1.66 (18H, s, $C(CH_3)_3$), 6.94 (1H, t, *p*-ArCH), 7.04 (2H, t, *m*-ArCH), 7.21 (2H, d, *o*-ArCH), 7.86 (2H, s, imidazole backbone CH), 8.81 (1H, s, C2H). $^{13}C\{^1H\}$ NMR (298 K, THF- d_8): δ 1.1 (CH_2SiMe_3), 3.5 ($Si(CH_3)_3$), 29.8 ($C(CH_3)_3$), 61.3 ($C(CH_3)_3$), 104.7 (PhC \equiv CGa), 105.4 (PhC \equiv CGa), 121.6 (imidazole backbone CH), 124.7 (*p*-ArCH), 128.1 (*m*-ArCH), 130.6 (ArC_{ipso}), 131.7 (*o*-ArCH), 132.3 (NCHN).

Synthesis of $[IPr-GaR_2(CCPH)]$ (24**).** Equimolar amounts of $Ga(CH_2SiMe_3)_3$ (0.165 g, 0.5 mmol) and IPr (0.2 g, 0.5 mmol) were suspended in 10 mL of hexane and stirred for 30 min at room temperature. An equivalent of phenylacetylene (51 mg, 55 μ L, 0.5 mmol) was added, and the obtained orange suspension was refluxed for 6 h. Slow cooling of the obtained orange solution afforded X-ray-quality crystals (189 mg, 55%). Anal. Calcd for $C_{43}H_{63}N_2Si_2Ga$: C, 70.38; H, 8.65; N, 3.82. Found: C, 69.32; H, 8.39; N, 3.59. 1H NMR (298 K, C_6D_6): δ -1.04 (4H, mult, CH_2SiMe_3), 0.30 (18H, s, $Si(CH_3)_3$), 0.97 (12H, d, $CH(CH_3)_2$), 1.45 (12H, d, $CH(CH_3)_2$), 2.84 (4H, sept, $CH(CH_3)_2$), 6.40 (2H, s, imidazole backbone CH), 6.98 (1H, t, *p*-ArCH, alkyne ligand), 7.09 (6H, mult, ArCH, Dipp ligand), 7.19 (2H, t, *m*-ArCH, alkyne ligand), 7.46 (2H, d, *o*-Ar-CH, alkyne ligand). $^{13}C\{^1H\}$ NMR (298 K, C_6D_6): δ -1.7(CH_2SiMe_3), 2.9 ($Si(CH_3)_3$), 23.0 ($CH(CH_3)_2$), 25.9 ($CH(CH_3)_2$), 28.9 ($CH(CH_3)_2$), 106.9 (PhC \equiv CGa), 112.5 (PhC \equiv CGa), 124.2 (ArCH), 124.6 (imidazole backbone CH), 126.0 (ArCH), 130.9 (ArCH), 131.7 (ArCH), 135.4 (ArC), 145.8 (ArC), 179.4 (CGa).

ASSOCIATED CONTENT

Supporting Information

The Supporting Information is available free of charge on the ACS Publications website at DOI: 10.1021/acs.inorgchem.7b00549.

Crystallographic details and copies of NMR spectra for compounds **7**, **8**, and **21–24** (PDF)

Accession Codes

CCDC 1545610–1545615 contain the supplementary crystallographic data for this paper. These data can be obtained free of charge via www.ccdc.cam.ac.uk/data_request/cif, by emailing data_request@ccdc.cam.ac.uk, or by contacting The Cambridge Crystallographic Data Centre, 12, Union Road, Cambridge CB2 1EZ, UK; fax: +44 1223 336033.

AUTHOR INFORMATION

Corresponding Author

*E-mail: eva.hevia@strath.ac.uk.

ORCID

Alan R. Kennedy: 0000-0003-3652-6015

Eva Hevia: 0000-0002-3998-7506

Notes

The authors declare no competing financial interest.

ACKNOWLEDGMENTS

We are extremely grateful to all of the co-workers whose names appear in the cited publications for their many valuable contributions to the development of this work. Professor Robert E. Mulvey deserves a special mention because, through an enjoyable collaboration with his group, we have established and extended the intriguing concept of TMT. We also thank him for his insightful comments and discussion during the production of this Forum Article. Funding is acknowledged from the European Research Council (ERC) MIXMETAPPS-279590 FP7 project and the EPSRC project “Towards a Paradigm Shift in the Principles and Practice of Polar Organometallic Chemistry”, grant number EP/N011384/1.

REFERENCES

- (1) (a) Clayden, J. *Organolithiums: Selectivity for Synthesis*; Elsevier: Oxford, U.K., 2002. (b) Schlosser, M. *Organometallics in Synthesis: Third Manual*, 2nd ed.; Wiley: Hoboken, NJ, 2013.
- (2) Knochel, P. *Handbook of Functionalized Organometallics*; Wiley-VCH: Weinheim, Germany, 2005; Vol. 1.
- (3) (a) Schlosser, M. The activation of organolithium reagents. *J. Organomet. Chem.* **1967**, *8*, 9. (b) Lochmann, L.; Pospisil, J.; Lim, D. On the interaction of organolithium compounds with sodium and potassium alkoxides. A new method for the synthesis of organosodium and organopotassium compounds. *Tetrahedron Lett.* **1966**, *7*, 257. (c) Benrath, P.; Kaiser, M.; Limbach, T.; Mondeshki, M.; Klett, J. Combining Neopentylolithium with Potassium *tert*-Butoxide: Formation of an Alkane-Soluble Lochmann–Schlosser Superbase. *Angew. Chem., Int. Ed.* **2016**, *55*, 10886.
- (4) (a) Uchiyama, M.; Koike, M.; Kameda, M.; Kondo, Y.; Sakamoto, T. Unique Reactivities of New Highly Coordinated Ate Complexes of Organozinc Derivatives. *J. Am. Chem. Soc.* **1996**, *118*, 8733. (b) Uchiyama, M.; Kameda, M.; Mishima, O.; Yokoyama, N.; Koike, M.; Kondo, Y.; Sakamoto, T. New Formulas for Organozincate Chemistry. *J. Am. Chem. Soc.* **1998**, *120*, 4934. (c) Kondo, Y.; Shilai, M.; Uchiyama, M.; Sakamoto, T. TMP–Zincate as Highly Chemoselective Base for Directed Ortho Metalation. *J. Am. Chem. Soc.* **1999**, *121*, 3539. (d) Uchiyama, M.; Furuyama, T.; Kobayashi, M.; Matsumoto, Y.; Tanaka, K. Toward a Protecting-Group-Free Halogen–Metal Exchange Reaction: Practical, Chemoselective Metalation of Functionalized Aromatic Halides Using Dianion-type Zincate, $t^iBu_4ZnLi_2$. *J. Am. Chem. Soc.* **2006**, *128*, 8404. (e) Furuyama, T.; Yonehara, M.; Arimoto, S.; Kobayashi, M.; Matsumoto, Y.; Uchiyama, M. Development of Highly Chemoselective Bulky Zincate Complex, $t^iBu_4ZnLi_2$: Design, Structure, and Practical Applications in Small-/Macromolecular Synthesis. *Chem. - Eur. J.* **2008**, *14*, 10348.
- (5) (a) Chau, N. T. T.; Meyer, M.; Komagawa, S.; Chevallier, F.; Fort, Y.; Uchiyama, M.; Mongin, F.; Gros, P. C. Homoleptic Zincate-Promoted Room-Temperature Halogen–Metal Exchange of Bromopyridines. *Chem. - Eur. J.* **2010**, *16*, 12425. (b) Snégárov, K.; Komagawa, S.; Chevallier, F.; Gros, P. C.; Golhen, S.; Roisnel, T.; Uchiyama, M.; Mongin, F. Deprotonative Metalation of Substituted Benzenes and Heteroaromatics Using Amino/Alkyl Mixed Lithium–Zinc Combinations. *Chem. - Eur. J.* **2010**, *16*, 8191.
- (6) (a) Krasovskiy, A.; Knochel, P. A LiCl-Mediated Br/Mg Exchange Reaction for the Preparation of Functionalized Aryl- and

- Heteroarylmagnesium Compounds from Organic Bromides. *Angew. Chem., Int. Ed.* **2004**, *43*, 3333. (b) Wunderlich, S. H.; Rohbogner, C. J.; Unsinn, A.; Knochel, P. Scalable Preparation of Functionalized Organometallics via Directed Ortho Metalation Using Mg- and Zn-Amide Bases. *Org. Process Res. Dev.* **2010**, *14*, 339. (c) Haag, B.; Mosrin, M.; Ila, H.; Malakhov, V.; Knochel, P. Regio- and Chemoselective Metalation of Arenes and Heteroarenes Using Hindered Metal Amide Bases. *Angew. Chem., Int. Ed.* **2011**, *50*, 9794. (d) Schnegelsberg, C.; Bachmann, S.; Kolter, M.; Auth, T.; John, M.; Stalke, D.; Koszinowski, K. Association and Dissociation of Grignard Reagents RMgCl and Their Turbo Variant RMgCl•LiCl. *Chem. - Eur. J.* **2016**, *22*, 7752. (e) Neufeld, R.; Teuteberg, T. L.; Herbst-Irmer, R.; Mata, R. A.; Stalke, D. Solution Structures of Hauser Base Pr_2NMgCl and Turbo-Hauser Base $\text{Pr}_2\text{NMgCl}\cdot\text{LiCl}$ in THF and the Influence of LiCl on the Schlenk-Equilibrium. *J. Am. Chem. Soc.* **2016**, *138*, 4796. (f) Bachmann, S.; Neufeld, R.; Dzemski, M.; Stalke, D. New External Calibration Curves (ECCs) for the Estimation of Molecular Weights in Various Common NMR Solvents. *Chem. - Eur. J.* **2016**, *22*, 8462.
- (7) (a) Andrikopoulos, P. C.; Armstrong, D. R.; Graham, D. V.; Hevia, E.; Kennedy, A. R.; Mulvey, R. E.; O'Hara, C. T.; Talmard, C. Selective Meta-Deprotonation of Toluene by Using Alkali-Metal-Mediated Magnesium. *Angew. Chem., Int. Ed.* **2005**, *44*, 3459. (b) Armstrong, D. R.; Clegg, W.; Dale, S. H.; Graham, D. V.; Hevia, E.; Hogg, L. M.; Honeyman, G. W.; Kennedy, A. R.; Mulvey, R. E. Dizincation and dimagnesiumation of benzene using alkali-metal-mediated metalation. *Chem. Commun.* **2007**, 598.
- (8) (a) Clegg, W.; Conway, B.; Graham, D. V.; Hevia, E.; Kennedy, A. R.; Mulvey, R. E.; Russo, L.; Wright, D. S. Structurally Defined Potassium-Mediated Zincation of Pyridine and 4-R-Substituted Pyridines (R = Et, *i*Pr, *t*Bu, Ph, and Me₂N) by Using Dialkyl-TMP-Zincate Bases. *Chem. - Eur. J.* **2009**, *15*, 7074. (b) Armstrong, D. R.; Blair, V. L.; Clegg, W.; Dale, S. H.; Garcia-Alvarez, J.; Honeyman, G. W.; Hevia, E.; Mulvey, R. E.; Russo, L. Structural Basis for Regioisomerization in the Alkali-Metal-Mediated Zincation (AMMzn) of Trifluoromethyl Benzene by Isolation of Kinetic and Thermodynamic Intermediates. *J. Am. Chem. Soc.* **2010**, *132*, 9480.
- (9) (a) Wunderlich, S. H.; Kienle, M.; Knochel, P. Directed Manganation of Functionalized Arenes and Heterocycles Using tmp₂Mn-2 MgCl₂-4 LiCl. *Angew. Chem., Int. Ed.* **2009**, *48*, 7256. (b) Garcia-Álvarez, J.; Kennedy, A. R.; Klett, J.; Mulvey, R. E. Alkali-Metal-Mediated Manganation: A Method for Directly Attaching Manganese(II) Centers to Aromatic Frameworks. *Angew. Chem., Int. Ed.* **2007**, *46*, 1105. (c) Blair, V. L.; Clegg, W.; Conway, B.; Hevia, E.; Kennedy, A. R.; Klett, J.; Mulvey, R. E.; Russo, L. Alkali-Metal-Mediated Manganation(II) of Functionalized Arenes and Applications of ortho-Manganated Products in Pd-Catalyzed Cross-Coupling Reactions with Iodobenzene. *Chem. - Eur. J.* **2008**, *14*, 65.
- (10) (a) Wunderlich, S. H.; Knochel, P. Preparation of Functionalized Aryl Iron(II) Compounds and a Nickel-Catalyzed Cross-Coupling with Alkyl Halides. *Angew. Chem., Int. Ed.* **2009**, *48*, 9717. (b) Alborés, P.; Carrella, L. M.; Clegg, W.; Garcia-Álvarez, P.; Kennedy, A. R.; Klett, J.; Mulvey, R. E.; Rentschler, E.; Russo, L. Direct C-H Metalation with Chromium(II) and Iron(II): Transition-Metal Host/Benzene Diene Guest Magnetic Inverse-Crown Complexes. *Angew. Chem., Int. Ed.* **2009**, *48*, 3317. (c) Nagaradja, E.; Chevallier, F.; Roisnel, T.; Jouikov, V.; Mongin, F. Deprotonative metalation of aromatic compounds using mixed lithium-iron combinations. *Tetrahedron* **2012**, *68*, 3063. (d) Bedford, R. B.; Brenner, P. B.; Carter, E.; Cogswell, P. M.; Haddow, M. F.; Harvey, J. N.; Murphy, D. M.; Nunn, J.; Woodall, C. H. TMEDA in Iron-Catalyzed Kumada Coupling: Amine Adduct versus Homoleptic "ate" Complex Formation. *Angew. Chem., Int. Ed.* **2014**, *53*, 1804.
- (11) Martínez-Martínez, A. J.; Kennedy, A. R.; Mulvey, R. E.; O'Hara, C. T. Directed ortho-meta' and meta-meta'-dimetalations: a template base approach to deprotonation. *Science* **2014**, *346*, 834.
- (12) Martínez-Martínez, A. J.; Fuentes, M. Á.; Hernán-Gómez, A.; Hevia, E.; Kennedy, A. R.; Mulvey, R. E.; O'Hara, C. T. Alkali-Metal-Mediated Magnesiumations of an N-Heterocyclic Carbene: Normal, Abnormal, and "Paranormal" Reactivity in a Single Tritopic Molecule. *Angew. Chem., Int. Ed.* **2015**, *54*, 14075.
- (13) For some recent reviews highlighting the applications of mixed-metal bases in deprotonative metalation, see: (a) Mulvey, R. E. Modern Ate Chemistry: Applications of Synergic Mixed Alkali-Metal-Magnesium or -Zinc Reagents in Synthesis and Structure Building. *Organometallics* **2006**, *25*, 1060. (b) Mulvey, R. E.; Mongin, F.; Uchiyama, M.; Kondo, Y. Deprotonative Metalation Using Ate Compounds: Synergy, Synthesis, and Structure Building. *Angew. Chem., Int. Ed.* **2007**, *46*, 3802. (c) Mulvey, R. E. Avant-Garde Metalating Agents: Structural Basis of Alkali-Metal-Mediated Metalation. *Acc. Chem. Res.* **2009**, *42*, 743. (d) Mulvey, R. E. An alternative picture of alkali-metal-mediated metalation: cleave and capture chemistry. *Dalton. Trans.* **2013**, *42*, 6676. (e) Harrison-Marchand, A.; Mongin, F. Mixed AggregAte (MAA): A Single Concept for All Dipolar Organometallic Aggregates. 1. Structural Data. *Chem. Rev.* **2013**, *113*, 7470. (f) Mongin, F.; Harrison-Marchand, A. Mixed AggregAte (MAA): A Single Concept for All Dipolar Organometallic Aggregates. 2. Syntheses and Reactivities of Homo/HeteroMAAs. *Chem. Rev.* **2013**, *113*, 7563.
- (14) Armstrong, D. R.; Crosbie, E.; Hevia, E.; Mulvey, R. E.; Ramsay, D. L.; Robertson, S. D. TMP (2,2,6,6-tetramethylpiperidide)-aluminate bases: lithium-mediated alumination or lithiation-alkylaluminum-trapping reagents? *Chem. Sci.* **2014**, *5*, 3031.
- (15) Mulvey, R. E.; Armstrong, D. R.; Conway, B.; Crosbie, E.; Kennedy, A. R.; Robertson, S. D. Structurally Powered Synergic 2,2,6,6-Tetramethylpiperidine Bimetallics: New Reflections through Lithium-Mediated Ortho Aluminations. *Inorg. Chem.* **2011**, *50*, 12241.
- (16) Clegg, W.; Crosbie, E.; Dale-Black, S. H.; Hevia, E.; Honeyman, G. W.; Kennedy, A. R.; Mulvey, R. E.; Ramsay, D. L.; Robertson, S. D. Structurally Defined Zincated and Aluminated Complexes of Ferrocene Made by Alkali-Metal Synergistic Syntheses. *Organometallics* **2015**, *34*, 2580.
- (17) Crosbie, E.; García-Álvarez, P.; Kennedy, A. R.; Klett, J.; Mulvey, R. E.; Robertson, S. D. Structurally Engineered Deprotonation/Alumination of THF and THTP with Retention of Their Cycloanionic Structures. *Angew. Chem., Int. Ed.* **2010**, *49*, 9388.
- (18) (a) Stephan, D. W.; Erker, G. Frustrated Lewis Pairs: Metal-free Hydrogen Activation and More. *Angew. Chem., Int. Ed.* **2010**, *49*, 46. (b) Stephan, D. W. Frustrated Lewis Pairs: From Concept to Catalysis. *Acc. Chem. Res.* **2015**, *48*, 306. (c) Stephan, D. W.; Erker, G. Frustrated Lewis Pair Chemistry: Development and Perspectives. *Angew. Chem., Int. Ed.* **2015**, *54*, 6400. (d) Erker, G.; Stephan, D. W. *Frustrated Lewis Pairs I: Uncovering and Understanding*; Springer: Berlin, 2013.
- (19) (a) Welch, G. C.; San Juan, R. R.; Masuda, J. D.; Stephan, D. W. Reversible, metal-free hydrogen activation. *Science* **2006**, *314*, 1124. (b) Holschumacher, D.; Bannenberg, T.; Hrib, C. G.; Jones, P. G.; Tamm, M. Heterolytic Dihydrogen Activation by a Frustrated Carbene-Borane Lewis Pair. *Angew. Chem., Int. Ed.* **2008**, *47*, 7428. (c) Chase, P. A.; Stephan, D. W. Hydrogen and Amine Activation by a Frustrated Lewis Pair of a Bulky N-Heterocyclic Carbene and B(C₆F₅)₃. *Angew. Chem., Int. Ed.* **2008**, *47*, 7433.
- (20) (a) Stephan, D. W. Frustrated Lewis pairs: a new strategy to small molecule activation and hydrogenation catalysis. *Dalton. Trans.* **2009**, 3129. (b) Hounjet, L. J.; Stephan, D. W. Hydrogenation by Frustrated Lewis Pairs: Main Group Alternatives to Transition Metal Catalysts? *Org. Process Res. Dev.* **2014**, *18*, 385.
- (21) (a) Mömmling, C. M.; Otten, E.; Kehr, G.; Fröhlich, R.; Grimme, S.; Stephan, D. W.; Erker, G. Reversible Metal-Free Carbon Dioxide Binding by Frustrated Lewis Pairs. *Angew. Chem., Int. Ed.* **2009**, *48*, 6643. (b) Ashley, A. E.; Thompson, A. L.; O'Hare, D. Non-Metal-Mediated Homogeneous Hydrogenation of CO₂ to CH₃OH. *Angew. Chem., Int. Ed.* **2009**, *48*, 9839. (c) Dureen, M. A.; Stephan, D. W. Reactions of Boron Amidinates with CO₂ and CO and Other Small Molecules. *J. Am. Chem. Soc.* **2010**, *132*, 13559. (d) Theuergarten, E.; Schlösser, J.; Schlüns, D.; Freytag, M.; Daniliuc, C. G.; Jones, P. G.; Tamm, M. Fixation of carbon dioxide and related small molecules by a bifunctional frustrated pyrazolylborane Lewis pair. *Dalton. Trans.* **2012**, *41*, 9101. (e) Sajid, M.; Kehr, G.; Daniliuc, C. G.; Erker, G.

Formylborane Formation with Frustrated Lewis Pair Templates. *Angew. Chem., Int. Ed.* **2014**, *53*, 1118. (f) Sajid, M.; Elmer, L.-M.; Rosorius, C.; Daniliuc, C. G.; Grimme, S.; Kehr, G.; Erker, G. Facile Carbon Monoxide Reduction at Intramolecular Frustrated Phosphane/Borane Lewis Pair Templates. *Angew. Chem., Int. Ed.* **2013**, *52*, 2243.

(22) (a) Axenov, K. V.; Mömning, C. M.; Kehr, G.; Fröhlich, R.; Erker, G. Structure and Dynamic Features of an Intramolecular Frustrated Lewis Pair. *Chem. - Eur. J.* **2010**, *16*, 14069. (b) Harhausen, M.; Fröhlich, R.; Kehr, G.; Erker, G. Reactions of Modified Intermolecular Frustrated P/B Lewis Pairs with Dihydrogen, Ethene, and Carbon Dioxide. *Organometallics* **2012**, *31*, 2801. (c) Sajid, M.; Klose, A.; Birkmann, B.; Liang, L.; Schirmer, B.; Wiegand, T.; Eckert, H.; Lough, A. J.; Fröhlich, R.; Daniliuc, C. G.; Grimme, S.; Stephan, D. W.; Kehr, G.; Erker, G. Reactions of phosphorus/boron frustrated Lewis pairs with SO₂. *Chem. Sci.* **2013**, *4*, 213. (d) Otten, E.; Neu, R. C.; Stephan, D. W. Complexation of Nitrous Oxide by Frustrated Lewis Pairs. *J. Am. Chem. Soc.* **2009**, *131*, 9918. (e) Neu, R. C.; Otten, E.; Lough, A.; Stephan, D. W. The synthesis and exchange chemistry of frustrated Lewis pair–nitrous oxide complexes. *Chem. Sci.* **2011**, *2*, 170.

(23) (a) Dureen, M. A.; Stephan, D. W. Terminal Alkyne Activation by Frustrated and Classical Lewis Acid/Phosphine Pairs. *J. Am. Chem. Soc.* **2009**, *131*, 8396. (b) Dureen, M. A.; Brown, C. C.; Stephan, D. W. Deprotonation and Addition Reactions of Frustrated Lewis Pairs with Alkynes. *Organometallics* **2010**, *29*, 6594. (c) Jiang, C.; Blacque, O.; Berke, H. Activation of Terminal Alkynes by Frustrated Lewis Pairs. *Organometallics* **2010**, *29*, 125.

(24) Mo, Z.; Rit, A.; Campos, J.; Kolychev, E. L.; Aldridge, S. Catalytic B–N Dehydrogenation Using Frustrated Lewis Pairs: Evidence for a Chain-Growth Coupling Mechanism. *J. Am. Chem. Soc.* **2016**, *138*, 3306.

(25) Hopkinson, M. N.; Richter, C.; Schedler, M.; Glorius, F. An overview of *N*-heterocyclic carbenes. *Nature* **2014**, *510*, 485.

(26) Kronig, S.; Theuergarten, E.; Holschumacher, D.; Bannenberg, T.; Daniliuc, C. G.; Jones, P. G.; Tamm, M. Dihydrogen Activation by Frustrated Carbene-Borane Lewis Pairs: An Experimental and Theoretical Study of Carbene Variation. *Inorg. Chem.* **2011**, *50*, 7344.

(27) (a) Appelt, C.; Westenberg, H.; Bertini, F.; Ehlers, A. W.; Slootweg, J. C.; Lammertsma, K.; Uhl, W. Geminal Phosphorus/Aluminum-Based Frustrated Lewis Pairs: C–H versus C≡C Activation and CO₂ Fixation. *Angew. Chem., Int. Ed.* **2011**, *50*, 3925. (b) Uhl, W.; Appelt, C.; Backs, J.; Westenberg, H.; Wollschläger, A.; Tannert, J. Al/P-Based Frustrated Lewis Pairs: Limitations of Their Synthesis by Hydroalumination and Formation of Dialkylaluminum Hydride Adducts. *Organometallics* **2014**, *33*, 1212. (c) Ménard, G.; Stephan, D. W. Room Temperature Reduction of CO₂ to Methanol by Al-Based Frustrated Lewis Pairs and Ammonia Borane. *J. Am. Chem. Soc.* **2010**, *132*, 1796. (d) Tai, C.-C.; Chang, Y.-T.; Tsai, J.-H.; Jurca, T.; Yap, G. P. A.; Ong, T. G. Subtle Reactivities of Boron and Aluminum Complexes with Amino-Linked *N*-Heterocyclic Carbene Ligation. *Organometallics* **2012**, *31*, 637. (e) Stennett, T. E.; Pahl, J.; Zijlstra, H. S.; Seidel, F. W.; Harder, S. A Frustrated Lewis Pair Based on a Cationic Aluminum Complex and Triphenylphosphine. *Organometallics* **2016**, *35*, 207. (f) Schnee, G.; Specklin, D.; Djukic, J.-P.; Dagorne, S. Deprotonation of Al₂Me₆ by Sterically Bulky NHCs: Scope, Rationale through DFT Studies, and Application in the Methylation of Carbonyl Substrates. *Organometallics* **2016**, *35*, 1726.

(28) (a) Abdalla, J. A. B.; Riddlstone, I. M.; Tirfoin, R.; Aldridge, S. Cooperative Bond Activation and Catalytic Reduction of Carbon Dioxide at a Group 13 Metal Center. *Angew. Chem., Int. Ed.* **2015**, *54*, 5098. (b) Uhl, W.; Tannert, J.; Layh, M.; Hepp, A.; Grimme, S.; Risthaus, T. Cooperative Ge–N Bond Activation in Hydrogallation Products of Alkynyl(diethylamino)germanes (Et₂N)_nGe(C≡C^tBu)_{4–n}. *Organometallics* **2013**, *32*, 6770. (c) Ganesamoorthy, C.; Matthias, M.; Bläser, D.; Wölper, C.; Schulz, S. Lewis acid–base adducts of group 13 elements: synthesis, structure and reactivity toward benzaldehyde. *Dalton Trans.* **2016**, *45*, 11437. (d) Uzelac, M.; Armstrong, D. R.; Kennedy, A. R.; Hevia, E. Understanding the

Subtleties of Frustrated Lewis Pair Activation of Carbonyl Compounds by *N*-Heterocyclic Carbene/Alkyl Gallium Pairings. *Chem. - Eur. J.* **2016**, *22*, 15826. (e) Backs, J.; Lange, M.; Possart, J.; Wollschläger, A.; Mück-Lichtenfeld, C.; Uhl, W. Facile Modulation of FLP Properties: A Phosphinylvinyl Grignard Reagent and Ga/P- and In/P₂-Based Frustrated Lewis Pairs. *Angew. Chem., Int. Ed.* **2017**, *56*, 3094.

(29) Martin, D.; Soleilhavoup, M.; Bertrand, G. Stable singlet carbenes as mimics for transition metal centers. *Chem. Sci.* **2011**, *2*, 389.

(30) (a) Spikes, G. H.; Fetting, J. C.; Power, P. P. Facile Activation of Dihydrogen by an Unsaturated Heavier Main Group Compound. *J. Am. Chem. Soc.* **2005**, *127*, 12232. (b) Summerscales, O. T.; Caputo, C. A.; Knapp, C. E.; Fetting, J. C.; Power, P. P. The Role of Group 14 Element Hydrides in the Activation of C–H Bonds in Cyclic Olefins. *J. Am. Chem. Soc.* **2012**, *134*, 14595. (c) Power, P. P. Main-group elements as transition metals. *Nature* **2010**, *463*, 171.

(31) Uzelac, M.; Kennedy, A. R.; Hevia, E.; Mulvey, R. E. Transforming LiTMP Lithiation of Challenging Diazines through Gallium Alkyl Trans-Metal-Trapping. *Angew. Chem., Int. Ed.* **2016**, *55*, 13147.

(32) Plé, N.; Turck, A.; Couture, K.; Quéguiner, G. Diazines 13: Metalation without Ortho-Directing Group - Functionalization of Diazines via Direct Metalation. *J. Org. Chem.* **1995**, *60*, 3781.

(33) Hilf, C.; Bosold, F.; Harms, K.; Marsch, M.; Boche, G. The Equilibrium Between 2-Lithium-Oxazole(-Thiazole, -Imidazole) Derivatives and Their Acyclic Isomers – A Structural Investigation. *Chem. Ber.* **1997**, *130*, 1213.

(34) (a) Jones, C.; Kennard, C. H. L.; Raston, C. L.; Smith, G. Negative hyperconjugation control of acidities in α -trimethylsilyl substituted α -picolines: isolation of [Li{NC₃H₂-2-C(H)(SiMe₃)₂}{NC₃H₂-2-C(H)(SiMe₃)₂}]₂. *J. Organomet. Chem.* **1990**, *396*, C39. (b) Leung, W.-P.; Weng, L.-H.; Wang, R.-J.; Mak, T. C. W. Synthesis and Crystal Structures of Lithium Complexes from the Metalation of 2-Picoline Derivatives. *Organometallics* **1995**, *14*, 4832. (c) Andrews, P. C.; Armstrong, D. R.; Raston, C. L.; Roberts, B. A.; Skelton, B. W.; White, A. H. Alkali metal and magnesium enamides from metalation of the alkyl ligands [(2-Pyr)(SiMe₃)CH₂] and [6-Me-(2-Pyr)(SiMe₃)CH₂]: a solid state and ab initio study. *J. Chem. Soc., Dalton Trans.* **2001**, 996. (d) Ott, H.; Pieper, U.; Leusser, D.; Flierler, U.; Henn, J.; Stalke, D. Carbanion or Amide? First Charge Density Study of Parent 2-Picolylithium. *Angew. Chem., Int. Ed.* **2009**, *48*, 2978. (e) Kennedy, A. R.; Mulvey, R. E.; Urquhart, R. I.; Robertson, S. D. Lithium, sodium and potassium picolyl complexes: syntheses, structures and bonding. *Dalton Trans.* **2014**, *43*, 14265.

(35) For a recent example of similar coordination of a 2-picolyl anion to a magnesium center, see: Davin, L.; McLellan, R.; Hernán-Gómez, A.; Clegg, W.; Kennedy, A. R.; Mertens, M.; Stepek, I. A.; Hevia, E. Regioselective magnesiation of *N*-heterocyclic molecules: securing insecure cyclic anions by a β -diketiminato-magnesium clamp. *Chem. Commun.* **2017**, *53*, 3653.

(36) This chemical shift compares well with that observed for the carbenic carbon in the NHC complex IPr-GaR₃ (see ref 38), at 186.6 ppm. This trend has also been observed in magnesiated benzimidazole complexes. See: (a) Baillie, S. E.; Blair, V. L.; Bradley, T. D.; Clegg, W.; Cowan, J.; Harrington, R. W.; Hernán-Gómez, A.; Kennedy, A. R.; Livingstone, Z.; Hevia, E. Isomeric and chemical consequences of the direct magnesiation of 1,3-benzoxazoles using β -diketiminato-stabilized magnesium bases. *Chem. Sci.* **2013**, *4*, 1895. (b) Armstrong, D. R.; Clegg, W.; Hernán-Gómez, A.; Kennedy, A. R.; Livingstone, Z.; Robertson, S. D.; Russo, L.; Hevia, E. Probing the metallating ability of a polybasic sodium alkylmagnesiate supported by a bulky bis(amido) ligand: deprotomagnesiation reactions of nitrogen-based aromatic substrates. *Dalton Trans.* **2014**, *43*, 4361.

(37) Armstrong, D. R.; Baillie, S. E.; Blair, V. L.; Chabloz, N. G.; Diez, J.; Garcia-Alvarez, J.; Kennedy, A. R.; Robertson, S. D.; Hevia, E. Alkali-metal-mediated zincation (AMMZn) meets *N*-heterocyclic carbene (NHC) chemistry: Zn–H exchange reactions and structural authentication of a dinuclear Au(I) complex with a NHC anion. *Chem. Sci.* **2013**, *4*, 4259.

(38) Uzelac, M.; Hernán-Gómez, A.; Armstrong, D. R.; Kennedy, A. R.; Hevia, E. Rational synthesis of normal, abnormal and anionic NHC–gallium alkyl complexes: structural, stability and isomerization insights. *Chem. Sci.* **2015**, *6*, 5719.

(39) Compound **10** can also be prepared by sequentially treating IPR with LiR (R = CH₂SiMe₃) and GaR₃.³⁸ This approach can also be extended to sodium and potassium.⁴⁰

(40) Uzelac, M.; Kennedy, A. R.; Hernán-Gómez, A.; Fuentes, M. Á.; Hevia, E. Heavier Alkali-metal Gallates as Platforms for Accessing Functionalized Abnormal NHC Carbene-Gallium Complexes. *Z. Anorg. Allg. Chem.* **2016**, *642*, 1241.

(41) (a) Guo, T.; Dechert, S.; Meyer, F. Dinuclear Palladium Complexes of Pyrazole-Bridged Bis(NHC) Ligands: A Delicate Balance between Normal and Abnormal Carbene Coordination. *Organometallics* **2014**, *33*, 5145. (b) Heckenroth, M.; Neels, A.; Garnier, M. G.; Aebi, P.; Ehlers, A. W.; Albrecht, M. On the Electronic Impact of Abnormal C4-Bonding in *N*-Heterocyclic Carbene Complexes. *Chem. - Eur. J.* **2009**, *15*, 9375. (c) Schmitt, A.-L.; Schnee, G.; Welter, R.; Dagonne, S. Unusual reactivity in organo-aluminum and NHC chemistry: deprotonation of AlMe₃ by an NHC moiety involving the formation of a sterically bulky NHC–AlMe₃ Lewis adduct. *Chem. Commun.* **2010**, *46*, 2480.

(42) Day, B. M.; Pugh, T.; Hendriks, D.; Guerra, C. F.; Evans, D. J.; Bickelhaupt, M. F.; Layfield, R. A. Normal-to-Abnormal Rearrangement and NHC Activation in Three-Coordinate Iron(II) Carbene Complexes. *J. Am. Chem. Soc.* **2013**, *135*, 13338.

(43) (a) Holschumacher, D.; Bannenberg, T.; Ibrum, K.; Daniliuc, C. G.; Jones, P. G.; Tamm, M. Selective heterolytic P–P bond cleavage of white phosphorus by a frustrated carbene-borane Lewis pair. *Dalton Trans.* **2010**, *39*, 10590. (b) Kolychev, E. L.; Bannenberg, T.; Freytag, M.; Daniliuc, C. G.; Jones, P. G.; Tamm, M. Reactivity of a Frustrated Lewis Pair and Small-Molecule Activation by an Isolable Arduengo Carbene–B{3,5-(CF₃)₂C₆H₃}₃ Complex. *Chem. - Eur. J.* **2012**, *18*, 16938.

(44) (a) Sumerin, V.; Schulz, F.; Nieger, M.; Leskelä, M.; Repo, T.; Rieger, B. Facile Heterolytic H₂ Activation by Amines and B(C₆F₅)₃. *Angew. Chem., Int. Ed.* **2008**, *47*, 6001. (b) Rokob, T. A.; Hamza, A.; Stirling, A.; Pápai, I. On the Mechanism of B(C₆F₅)₃-Catalyzed Direct Hydrogenation of Imines: Inherent and Thermally Induced Frustration. *J. Am. Chem. Soc.* **2009**, *131*, 2029. (c) Bagutski, V.; Del Grosso, A.; Carrillo, J. A.; Cade, I. A.; Helm, M. D.; Lawson, J. R.; Singleton, P. J.; Solomon, S. A.; Marcelli, T.; Ingleson, M. J. Mechanistic Studies into Amine-Mediated Electrophilic Arene Borylation and Its Application in MIDA Boronate Synthesis. *J. Am. Chem. Soc.* **2013**, *135*, 474.

(45) (a) Horeglad, P.; Abilalimov, O.; Szczepaniak, G.; Dabrowska, A. M.; Dranka, M.; Zachara, J. Dialkylgallium Complexes with Alkoxide and Aryloxy Ligands Possessing *N*-Heterocyclic Carbene Functionalities: Synthesis and Structure. *Organometallics* **2014**, *33*, 100. (b) Horeglad, P.; Cybularczyk, M.; Trzaskowski, B.; Zukowska, G. Z.; Dranka, M.; Zachara, J. Dialkylgallium Alkoxides Stabilized with *N*-Heterocyclic Carbenes: Opportunities and Limitations for the Controlled and Stereoselective Polymerization of *rac*-Lactide. *Organometallics* **2015**, *34*, 3480.

(46) Gomez-Pantoja, M.; Gomez-Sal, P.; Hernan-Gomez, A.; Martin, A.; Mena, M.; Santamaria, C. Co-complexation of Lithium Gallates on the Titanium Molecular Oxide {[Ti(η⁵-C₅Me₅)(μ-O)}₃(μ₃-CH)]. *Inorg. Chem.* **2012**, *51*, 8964.

(47) (a) Schiefer, M.; Reddy, N. D.; Ahn, H.-J.; Stasch, A.; Roesky, H. W.; Schlicker, A. C.; Schmidt, H.-G.; Noltemeyer, M.; Vidovic, D. Neutral and Ionic Aluminum, Gallium, and Indium Compounds Carrying Two or Three Terminal Ethynyl Groups. *Inorg. Chem.* **2003**, *42*, 4970. (b) Uhl, W.; Spies, T. Reactions of the Dielement Compounds R₂E-ER₂ [E = Ga, In; R = CH(SiMe₃)₂] with Lithium Phenylethyne - Formation of Adducts by Retention of the E-E Bonds. *Z. Anorg. Allg. Chem.* **2000**, *626*, 1059. (c) Uhl, W.; Breher, F.; Haddadpour, S.; Koch, R.; Matar, M. Two Different Structural Motifs Observed for Dimeric Dialkylaluminum and Dialkylgallium Alkynides [R₂E-C≡C-C₆H₅]₂. *Z. Anorg. Allg. Chem.* **2004**, *630*, 1839. (d) Chmiel,

J.; Neumann, B.; Stammler, H.-G.; Mitzel, N. W. Dialkylaluminum-, -Gallium-, and -Indium-Based Poly-Lewis Acids with a 1,8-Diethynylanthracene Backbone. *Chem. - Eur. J.* **2010**, *16*, 11906.

(48) Winkelhaus, D.; Neumann, B.; Stammler, H.-G.; Mitzel, N. W. Intramolecular Lewis acid–base pairs based on 4-ethynyl-2,6-lutidine. *Dalton. Trans.* **2012**, *41*, 9143.

(49) Uhl, W.; Willeke, M.; Hengesbach, F.; Hepp, A.; Layh, M. Aluminium and Gallium Hydrazides as Active Lewis Pairs: Cooperative C-H Bond Activation with H-C≡C-Ph and Pentafluorobenzene. *Organometallics* **2016**, *35*, 3701.

(50) The heating of isolated compound **24** with 2 equiv of phenylacetylene in C₆D₆ at 100 °C resulted in the replacement of the second R group (now detected as TMS) with the alkynyl ligand; however, this required long heating times (46 h). Further heating at 100 °C for 23 h showed no signs of activation of the third arm. This is in line with the reactivity observed by Uhl and co-workers,⁴⁹ where GaMe₃ reacted with all three arms whereas Ga^tBu₃ reacted only with one arm.

(51) Dennis, L. M.; Patnode, W. Gallium triethyl monoetherate, gallium triethyl, gallium trimethylamine. *J. Am. Chem. Soc.* **1932**, *54*, 182.

(52) Hurst, E. C.; Wilson, K.; Fairlamb, I. J.; Chechik, V. *N*-Heterocyclic carbene coated metal nanoparticles. *New J. Chem.* **2009**, *33*, 1837.

(53) Hevia, E.; Kennedy, A. R.; Mulvey, R. E.; Ramsay, D. L.; Robertson, S. D. Concealed Cyclotrimeric Polymorph of Lithium 2,2,6,6-Tetramethylpiperidine Unconcealed: X-Ray Crystallographic and NMR Spectroscopic Studies. *Chem. - Eur. J.* **2013**, *19*, 14069.